Self-consistent-field calculation of structures and static properties of the solid-fluid interface: Paraffinlike molecule systems

Xiang-Yang Liu and P. Bennema
Research Institute for Materials, Laboratory of Solid State Chemistry, Faculty of Science, University of Nijmegen, Toernooiveld, 6525 ED Nijmegen, The Netherlands
(Received 7 April 1993)

The interfacial structure and interfacial properties were investigated within the framework of an inhomogeneous cell model, using self-consistent-field calculations. For interfacial systems consisting of completely flexible chain molecules, profiles of the segment density of fluid molecules vanish exponentially versus distance z from the solid surface. It can be shown that the structure of the solid-fluid interface can be characterized by two key factors: the surface scaling factor C_l^* and the characteristic thickness of the interface n^*. In contrast, the exponential law cannot be applied to interfacial systems consisting of molecules with somewhat rigid chains. For those systems, the ordering and the layering of chain molecules occur at the solid-fluid interface, due to the energy and the entropy effect. In addition to the factor C_l^*, the structure of the solid-fluid interface of the system may qualitatively be related to half of the chain length of solute molecules and of solvent molecules. Finally, the calculated values of C_l^* are compared with the experimental ones for a variety of n-paraffin systems. The results are very satisfactory.

PACS number(s): 68.45.−v, 68.15.+e, 36.20.Ey, 61.41.+e

I. INTRODUCTION

In this study, the description of the solid-fluid interface is within the framework of our inhomogeneous cell model developed recently [1–4]. The results are obtained from calculations of self-consistent-field (SCF) theories and can be seen as applications and extensions of our model. The subject of the solid-fluid interface has important implications for different fields, such as polymer and colloid science, catalysis, crystal growth, etc. However, in this paper we only concentrate on those issues which may be related to the growth of crystals. In these cases, crystal surfaces are in contact with a solution or the melt. Following from recent investigations, more attention is paid to problems of the morphology and growth of n-paraffin crystals in solutions (or the melt) [5,6]. First, the study of the morphology of normal paraffin crystals has practical implications. Many of the products derived from crude petroleum contain n-paraffins and these waxes can cause severe problems if they are allowed to crystallize. Crude oil, heavy fuel, diesel fuel, heating oil, etc., all contain significant proportions of higher n-paraffins. If the temperature drops abruptly during the winter, these paraffins crystallize as thin, flat plates. Those platy paraffin crystals which are present in every system can gel the fuel or block pipes and filters. To solve this problem, additives are developed, which change the habit of these crystals and significantly decrease their sizes so that they no longer suffer from the drawbacks mentioned above. Certainly, those additives must have a significant influence on the structure of the solid-fluid interface, hence on the morphology of crystals. In this sense, to understand the influence of additives on the interfacial structure will be a key step for molecular design of tailor-made additives. Second, it was found [7,8] that a first-order roughening transition occurs on surfaces of paraffin crystals when they are grown from n-hexane solutions. In case aromatic solvents are chosen, the order of surface roughening may be changed from first order to infinite order [9]. These novel phenomena are of theoretical and practical importance, and are also directly related to the structure and properties of the solid-fluid interface.

Paraffin systems are also considered as intermediate systems which bridge the gap between small molecule systems (i.e., monomer systems) and macromolecule systems (i.e., polymer systems). Therefore, a better understanding of crystal interfaces of paraffins is of particular practical and scientific interest for both small molecular and macromolecular crystals.

Early theoretical studies on the structure and static properties of the solid-fluid interface treated mostly simple fluids [10–16], while more recently increased attention has been focused on molecularly complex systems [17–19]. However, for complex molecule systems, such as polymers, molecules with flexible chains are the major subject. There are not many reports on paraffin systems.

In this study, interfacial systems of paraffinlike molecules, especially crystals in contact with solutions or the melt, are treated. Within the framework of the inhomogeneous cell model, the structure of the interface is calculated by the SCF theory of Scheutjens and co-workers [20–23]. This approach, similar to our formalisms of the solid-fluid interface [1–4], is based on the principles of cell models. So the results obtained can easily be interpreted by our interfacial model. This paper will be organized as follows. In Sec. II we will briefly introduce the interfacial model and the principles of the SCF calculations. The results of the interfacial structure and detailed interpretations will be given in Sec. III. This is to gain physical insight into the interface of paraffin systems. Finally, some conclusions are presented in Sec. IV.

II. THE INTERFACIAL MODEL AND THE SCF CALCULATION

A. The interfacial inhomogeneous cell model

In our previous papers [2–4], a so-called inhomogeneous cell model was developed to describe the solid-fluid interface. Within the framework of this model, the Cartesian coordinate system is defined in the following way: the x and y axes are in the plane of the solid surface, the z axis is normal to the surface, and the origin is in the center of the first fluid layer. According to cell models [24], the whole space is divided into cells of the same shape and size. In addition to this, in our inhomogeneous cell model the same type of cells (or units) are characterized by the distance (z) to the solid surface. This implies that the same types of cells will be in different environments if the distance z is different. It follows that physical properties of cells depend also on the distance z. Since the equilibrium state is taken into account, most or all cells are in mutual equilibrium and their chemical potentials are constant. Suppose that each structural unit is connected by the bonds $i=1,2,\ldots,m$ to neighboring units. Using the language of regular solution theories [3,24], the exchange bond energy ϕ_i (per mode) in the direction i is expressed for crystals in contact with a two-component solution, as

$$\phi_i(z)\simeq\tfrac{1}{2}[\phi^{AA}(z)-\phi_i^{SS}(-z)] +[1-X_A(z)]^2\phi_i^{\sigma}(z) \tag{1}$$

and

$$\phi_i^{\sigma}(z)=\phi_i^{AA}(z)-\tfrac{1}{2}[\phi_i^{AA}(z)+\phi_i^{BB}(z)] , \tag{1'}$$

where superscripts A, B, and S denote solute, solvent, and solid; AA, BB, AB, and SS denote solute-solute, solvent-solvent, solute-solvent, and solid-solid interactions, respectively; and $X_A(z)$ is the concentration of solute in layer z. The molar enthalpy of dissolution is given by

$$\Delta h_d(z)=\sum_{i=1}^{m}\phi_i(z) . \tag{2}$$

Note that $\phi_i(0)$ and $\Delta h_d(0)$ correspond to $\phi_i(z)$ and $\Delta h_d(z)$ in the first interfacial layer, and ϕ_i and Δh_d to those in the bulk.

In order to calculate the bond energies $\phi_i(z)$ from experimental data, the traditional proportionality assumption [6,25] is introduced. This implies that for a structural unit in a layer at a distance z away from the solid surface, the following relation is supposed to hold:

$$\phi_1(z):\phi_2(z):\cdots:\phi_i(z):\cdots:\phi_m(z) =\phi_1^{SS}:\phi_2^{SS}:\cdots:\phi_1^{SS}:\cdots\phi_m^{SS} . \tag{3}$$

(Here ϕ_1^{SS} represents the solid-solid bond energies of the bulk phase in the direction i.) In other words, for the bond energies $\phi_i(z)$ occurring in any environment, the ratio of bond energies is the same as the ratio of the bond energies ϕ_i^{SS}. ϕ_1^{SS} can in principle be calculated from a given crystal structure. Then $\phi_i(z)$ may also be calculated if $\Delta h_d(z)$ is available. (Normally, only Δh_d is available from solubility data.)

As mentioned earlier, the exchange bond energy in the first interfacial fluid layer is important for physical processes occurring on the crystal surface. In the connection of $\phi_i(0)$ with ϕ_i, a so-called surface characteristic scaling factor C_l^* was introduced [1,2],

$$C_l^*=\frac{\Delta h_d(0)}{\Delta h_d}\simeq\frac{\phi_i(0)}{\phi_i} . \tag{4}$$

This factor can be related to the concentration of solute for regular solutions as [2]

$$C_l^*\simeq\ln X_A(0)/\ln X_A . \tag{4'}$$

[X_A is the concentration of solute in the bulk, $X_A(0)$ is that in the first fluid layer adjacent to the solid phase.] Actually, the factor C_l^* is used to characterize the solid-fluid interface [1,2]. If $C_l^*=1$ [$X_A(0)=X_A$], the so-called equivalent wetting occurs on the solid surface. Otherwise, if $C_l^*<1$ [$X_A(0)>X_A$], or $C_l^*>1$ [$X_A(0)<X_A$], the so-called more than equivalent wetting case or the less than equivalent wetting case occurs, respectively. The equivalent wetting corresponds to the case that the structure and properties of a phase are homogeneous from the bulk up to the dividing plane between the solid and the fluid phase. We consider this as a reference state, and it will occur only in some very particular cases. The more than equivalent wetting (or the less than equivalent wetting) implies that the crystal surface shows an adsorption (or a desorption) to solute units. In normal cases, the nonequivalent wetting will occur in solid-fluid interfacial systems.

Experimentally, the factor C_l^* can also be determined. First, ϕ_i may be calculated based on (2) and (3). $\phi_i(0)$ can be determined from experiments of roughening transitions of crystal surfaces [5–7]. The roughening transition is a phase transition occurring at a crystal surface at the roughening temperature. If the temperature T is lower than the roughening temperature T^r of the crystal surface, the crystal surface is flat on a molecular scale at equilibrium. If $T\geq T^r$, the crystal surface roughens on a molecular scale [5–7]. According to the definition of the dimensionless roughening temperature,

$$\Theta_{hkl}^r=\frac{2kT^r}{\phi_i(0)} , \tag{5}$$

the roughening temperature T^r is directly related to the interfacial bond energy $\phi_i(0)$. Here Θ_{hkl}^r is the dimensionless roughening temperature of crystal faces $\{hkl\}$ and the value can be calculated by a computer program [6], k is the Boltzmann constant. Therefore, $\phi_i(0)$ can be determined by measuring the roughening temperature of the crystal surface T^r. Alternatively, assuming that the step free energy is approximately equal to the step energy, $\phi_i(0)$ can also be measured by fitting the data of growth rate R versus the supersaturation β, according to a two-dimensional nucleation growth mechanism (a birth and spread mechanism [25]), by

$$R = A'\beta^{5/6}\exp(B'/\beta) \tag{6}$$

where A' is a kinetic constant and

$$B' \simeq f[\phi_i(0)]^2 , \tag{6'}$$

where f is a factor depending on the shape of nuclei, the temperature, and structural parameters of crystal surfaces, and can be calculated for a given crystal surface structure. As soon as B' is obtained from experiments, $\phi_i(0)$ can be calculated according to (6'). On the other hand, in case the concentration at the interface can be calculated or measured, C_l^* can also be obtained using (4'). In the following, it will be shown that C_l^* can be calculated according to (4') for various systems, using SCF calculations.

Concerning the structure of the solid-fluid interface, profiles of the concentration, for systems consisting of isotropic structural units, obey an exponential law [3]. This implies that

$$X_A(z) = X_A\{1 + D\exp[-z/(n^*d)]\} , \tag{7}$$

where

$$D = X_A^{\zeta} - 1 , \quad \zeta = C_l^* - 1 . \tag{7'}$$

Here d is the interplanar thickness of the solid in the orientations $\{hkl\}$ and n^* is the normalized characteristic thickness of the interface, which is defined in such a way that at $z = n^*d$, $[X_A(z) - X_A]/(X_A D) = \exp(-1)$. Note that in this approach [3], the mean-field approximation is applied. This means that fluctuations of the density within a layer are neglected. It follows that Eq. (7) represents an average profile of the density at the interface. It can be seen from (7) that interfacial profiles of the density will be fixed if X_A, C_l^*, and n^* are given. Obviously, since X_A is always available, the values of C_l^* and n^* are the most important to characterize the structure.

B. The self-consistent-field theory calculation

The SCF theory developed by Scheutjens and Fleer [20] is also based on a cell model. Similar to the above-mentioned inhomogeneous model, the space is divided in lattice layers parallel to the solid surface. A molecule of type i has a volume fraction $\varphi_i(z)$ in layer z and φ_i in the bulk solution. Only inhomogeneities perpendicular to the surface are considered. Since the mean-field approximation is applied in the calculation, fluctuations with the lattice layers are also neglected. A chain molecule consists of r segments, and fills r lattice sites. In the case of paraffin solutions, it is assumed that chain molecules are homogeneous (all segments of a molecule are of the same type), and molecules with longer chains are solute molecules (denoted by A) and molecules with shorter chains are solvent molecules (denoted by B).

For n-paraffin crystals in contact with paraffin solutions, the exchange energy per segment between n-paraffin A and n-paraffin B is supposed to be zero. The interaction between a segment i ($i = A$ or B) and a surface site is expressed by the Flory-Huggin parameter χ_{si} ($i = A$ or B). This parameter is expressed in units of kT and corresponds to the energy changed (per segment) due to bringing a segment i from the pure liquid state i into an environment of the pure solid state s. In the case of growth of paraffin crystals, substrates are the solid paraffins. Then, for n-paraffin crystals with the orthorhombic structure, $\chi_{si} \simeq -1.54 + 6.0/r$ and for the triclinic structure $\chi_{si} \simeq -1.63 + 4.69/r$ [26]. If it is not specified, χ_{si} is referenced to $T = 298.15$ K.

Due to the energy difference between the *trans* conformation and the *gauche* conformation of molecular chains, there are some torsional energies ε^{tor} in carbon chains of n-paraffin molecules. In the calculations, this can also be considered. For the formalisms and other calculation details, see Refs. [20–23].

III. RESULTS AND DISCUSSION

A. Molecules with completely flexible chains

Polymer molecules are in many cases treated as flexible molecules. However, under conditions of crystal growth, paraffin molecules are considered to be somewhat rigid molecules. In connection with polymer systems, we will first consider paraffin molecules to be flexible.

Solute and solvent molecules are denoted by C_r and C_r', respectively. Since in this case chain molecules are fully flexible, they can be considered as isotropic structural units. Therefore, profiles of the concentration will obey the exponential law. In Fig. 1, a linear relation between $\ln[X_A(z) - X_A]$ and z for systems of C_{36} in C_6' solutions is presented. [Note that the calculated volume fractions $\varphi(z)$ are converted into molar fractions $X_A(z)$]. It is known from the last section that in this case the structure of the solid-fluid interface can be characterized by the two factors C_l^* and n^*. Hence, we will in the following

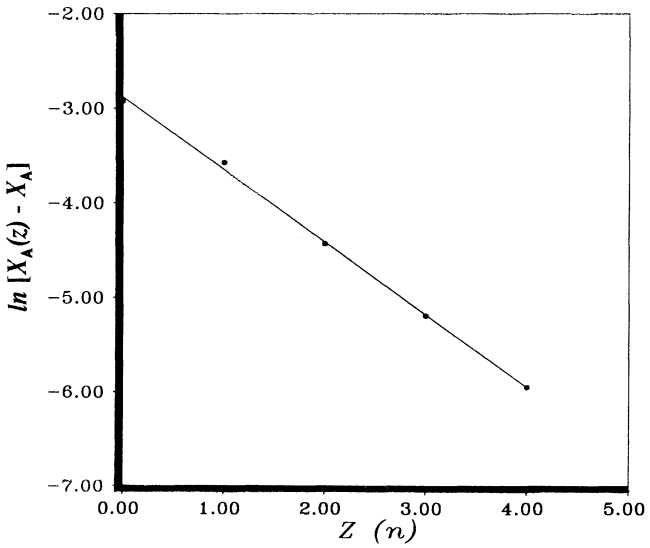

FIG. 1. The linear relation between $\ln[X_A(z) - X_A]$ and the distance z for systems of C_{36}-C_6' solution. X_A: the mole fraction of solute; the lattice structure is hexagonal; $\varphi_A = 0.1$.

discuss the influence of the chain length and the concentration of solute molecules on those two factors.

In Fig. 2, the dependence of C_l^* and n^* on the chain length of solute molecules for C_6' solution systems are shown, respectively. It can be seen from Fig. 2(a) that $C_l^* < 1$. This means that the more than equivalent wetting case occurs in chain molecule systems. It can also be seen that C_l^* decreases further from unity with the segment number of solute molecules. In contrast, n^* is increasing with the segment number. This suggests that with increasing segment number, solute molecules are more strongly adsorbed on the solid surface, and that the solid-fluid interface will become somewhat thicker.

For a system with a given solute and a given solvent, the structure of the solid-fluid interface can also be influenced by the bulk concentration of the solution. An example of this influence is displayed in Fig. 3. As shown in Figs. 3(a) and 3(b) both C_l^* and n^* decrease with the concentration of solute. These parallel changes of C_l^* and n^* are different from those shown in Figs. 2(a) and 2(b). The results of Fig. 3 mean that when the concentration increases, solute molecules show stronger tendencies to be adsorbed at the solid surface. However, the solid-fluid interface becomes thinner. We notice that for monomer systems, only n^* is influenced by the concentration. C_l^* is independent of X_A. (This result will be published elsewhere.)

In addition to Fig. 3, segmental profiles of the concen-

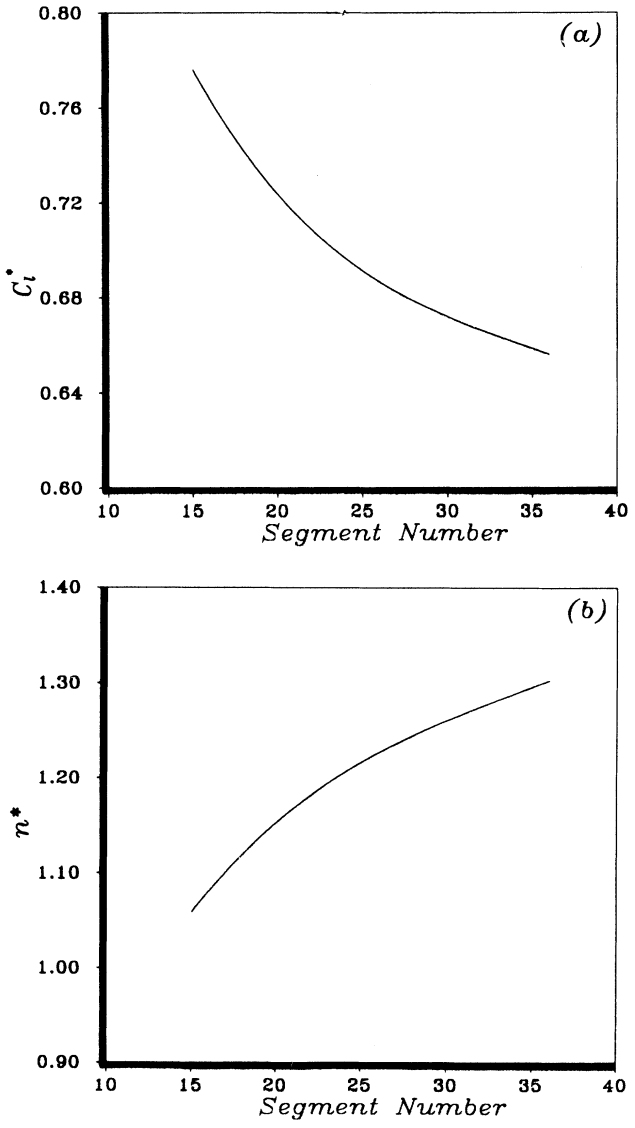

FIG. 2. The influence of the chain length of solute molecules on the interfacial structure. (a) The relation between the factor C_l^* and the chain length. (b) The relation between the characteristic thickness of interfaces n^* and the chain length. Solvent: C_6'; $\varphi_A = 0.1$; the lattice structure is hexagonal.

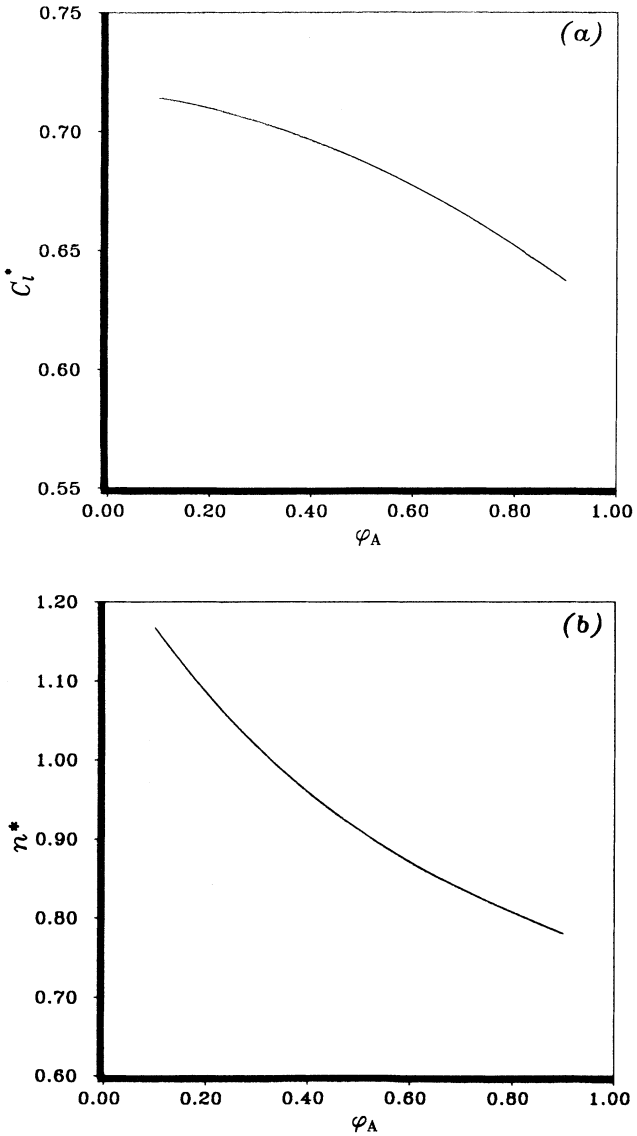

FIG. 3. The influence of the bulk concentration of solute on the interfacial structure. (a) The dependence of C_l^* on the concentration. (b) The dependence of n^* on the concentration. System: $C_{21} + C_6'$; the lattice structure is hexagonal.

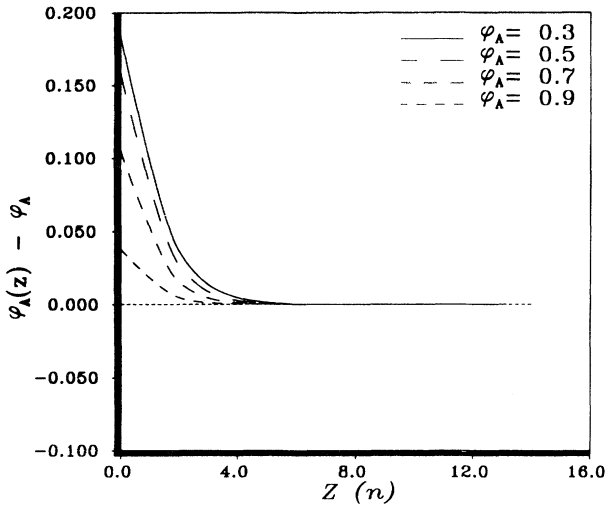

FIG. 4. Exponential profiles of the relative segment density $[\varphi_A(z)-\varphi_A]$, plotted as a function of the distance z, for various bulk concentrations. Relevant parameters: the same as Fig. 3.

tration of solute [expressed by the volume fraction $\varphi_A(z)$] are plotted versus the distance away from the solid surface for various concentrations, and presented in Fig. 4.

B. Molecules with rigid chains

In the case of paraffin molecules, molecular chains are not completely flexible. It follows that the torsional energy of C—C chains should be taken into consideration in the calculations. This will lead to some particular results. In the following, we will first concentrate on the problems of the ordering and the structuring of the interface due to the rigidity of molecular chains. Then discussions on the wetting condition and the influence on interfacial properties are given later.

1. Ordering of molecules at the interface

The torsional energy ε^{tor} of C—C chains is due to the energy difference between the *trans* and the *gauche* conformation of molecules. This energy for normal paraffin molecules is about $2kT_0$ [27]. In comparison with Fig. 4, the profile of the concentration of n-C_{21} $\varphi_A(z)$ in an n-C_6 solution ($\varphi_A=0.1$, $\varepsilon^{\text{tor}}=2kT_0$) is plotted versus distance z from the first fluid layer ($z=0$) (see Fig. 5). It can be seen from Fig. 5 that for rigid-chain molecules, since the anisotropy occurs in the molecular structure, the exponential law cannot be applied to the system. Instead, $\varphi_A(z)$ shows an oscillatory decrease. This leads to the concentration depletion of the solute between the first fluid layer and the layer $z=\lambda_0$ where $\varphi_A(\lambda_0)\simeq\varphi_A$.

It is interesting to see from our calculations that for rigid-chain molecular systems, the position of λ_0 (or $\lambda_{\max}$) and the position of the first minimum of $\varphi_A(z)$ (at $z=\lambda_{\min}$) are directly associated with the structure of solute molecules and of solvent molecules. For completely rigid molecular solution systems, a maximum of $\varphi_A(z)$ occurs in the layer $z=\lambda_{\max}$ after the first fluid layer, and $\lambda_{\max}$ corresponds to half of the change length of solute molecules λ_A, whereas $\lambda_{\min}$ corresponds to half of the chain length of solvent molecules. In the case of normal alkaline molecules, molecular chains are not completely rigid ($\varepsilon^{\text{tor}}\simeq 2kT_0$), then $\lambda_{\max}$ is replaced by λ_0. Due to the lagging of $\varphi_A(z)$, it turns out for the n-paraffin solution system that $\lambda_{\min}\simeq\lambda'_B\simeq\lambda_B+3$ and $\lambda_0\simeq\lambda'_A\simeq\lambda_A+3$. These results are explicitly shown in Fig. 6. From this point of view, the structure of the solid-fluid interface explicitly depends on the structure of paraffinlike molecules.

For crystals in contact with the melt (assuming $\varphi_A\simeq\rho_f/\rho_s$, ρ_f and ρ_s are the density of the melt and the solid [2]), the oscillation also does occur in profiles of the segmental density. However, the profiles are characterized by $z=\lambda_{\max}\simeq\lambda_A$ since molecules of one kind exist in the system. It follows that the profiles will be smoothed if the temperature increases (see Fig. 7).

In order to characterize the ordering of chain molecules, a segment order parameter [23] is defined as

$$s=(3\langle\cos^2\alpha\rangle-1)/2\ , \tag{8}$$

where α is the angle between the axis of an unit and a given direction. Here, the orientation of segments occurs with respect to the normal to the solid surface. For a certain species, the order parameter $s(z)$ is a function of z. In the case of a chain molecule, we use $\bar{s}(z)$, which is the ensemble average over all segments of the molecule, to characterize the ordering of this molecule. It is explicit that in case that all bonds of the molecule are completely parallel to the surface, the order parameter is -0.5. If all of the bonds are perpendicular to the surface, $s(z)=1$. On the other hand, a random distribution of bonds will result in the order parameter $s(z)=0$ [23]. It follows that

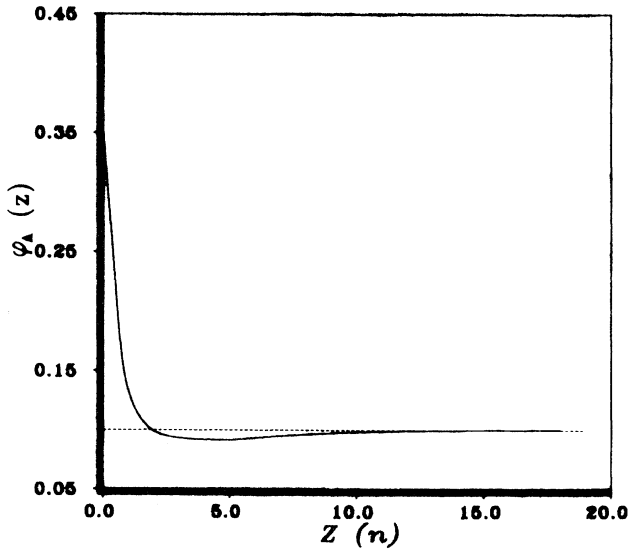

FIG. 5. Segment-density profile $\varphi_A(z)$ of n-C_{21} molecules in an n-C_6 solution plotted versus distance z from the solid surface, with the origin at the center of the first fluid layer adjacent to the solid substrate. The segment density in the bulk $\varphi_A=0.1$, $\varepsilon^{\text{tor}}=2kT_0$, $T=T_0=298.15$ K. The lattice structure is fcc.

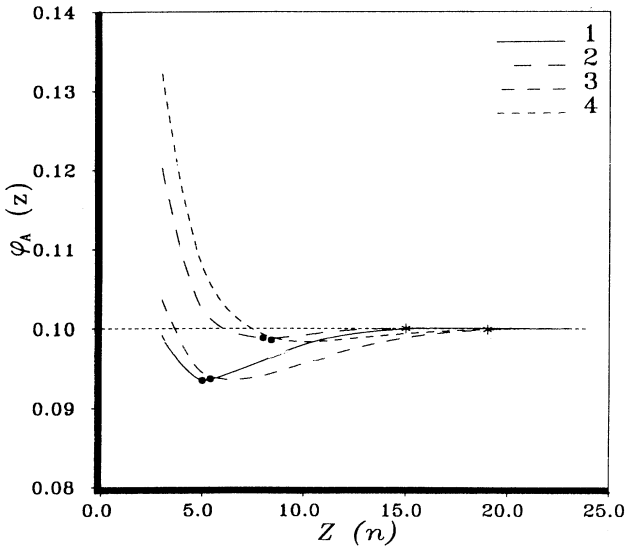

FIG. 6. Segment-density profiles in dependence of the structure of chain molecules. The structure of substrates is hexagonal; $\varphi_A=0.1$, $\varepsilon^{tor}=2kT_0$. Curve 1: n-$C_{23}+n$-C_6; curve 2: n-$C_{23}+n$-C_{12}; curve 3: n-$C_{33}+n$-C_6; curve 4: n-$C_{33}+n$-C_{12}. The positions of λ_{min}(●) and those of λ_0(*) are associated with the chain length of solute molecules and of solvent molecules, respectively.

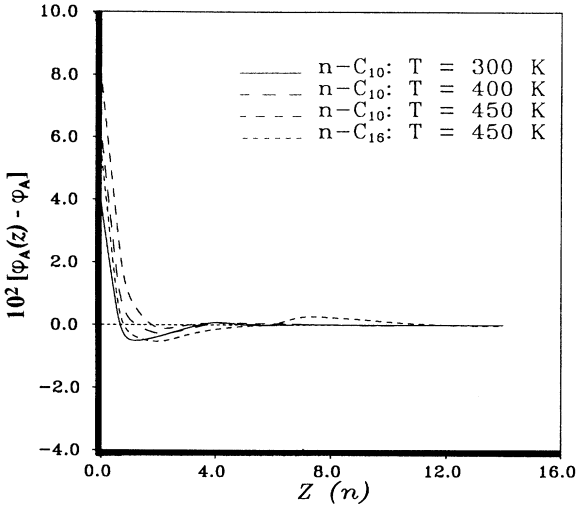

FIG. 7. Profiles of the relative segment density $[(\varphi_A(z)-\varphi_A),\varphi_A\simeq\rho_f/\rho_s]$ for different paraffin melt (n-C_{10}, n-C_{16}) systems, and the dependence of the profiles for an n-C_{10} system on the temperature: $\varepsilon^{tor}\simeq 1$ kcal/mol. For n-C_{16} systems, $T=450$ K, $\rho_f/\rho_s\simeq 0.80$; for n-C_{10}, $T=300$, 400, 450 K, then $\rho_f/\rho_s\simeq 0.900$, 0.798, 0.738, respectively. Note that the profiles are characterized by $z=\lambda_{max}\simeq\lambda_A$, and the oscillations are smoothed with increasing the temperature. The lattice structure is fcc.

at the solid surface, the order parameter should be very close to -0.5 if molecules are highly ordered (parallel to the surface). In Fig. 8, the values of $\bar{s}(z)$ are given as a function of z, for a C_{16}-C_6' solution system with different torsional energies of molecular chains ε^{tor}. It can be seen first that in any case, both solute and solvent molecules are preferentially adsorbed parallel to the solid surface in the first fluid layer. After the first fluid layer, the order parameter is increasing considerably, meaning that the degree of ordering is drastically reduced. In spite of this, chains with various torsional energies show a different behavior. Comparing with rigid-chain molecules ($\varepsilon^{tor}>0$), molecules with completely flexible chains ($\varepsilon^{tor}=0$) are less ordered, and in this case there is almost no difference between long-chain molecules and short-chain molecules [see Fig. 8(a)]. As a result, loops occur in those adsorbed flexible molecular chains. This can be seen from Fig. 8(a) that a positive peak occurs in the second fluid layer. With increasing torsional energy ε^{tor}, chain molecules are more preferentially adsorbed parallel to the solid surface. Also, longer-chain molecules are more ordered than short-chain molecules. These results can be seen from Figs. 8(b)–8(d), which correspond to $\varepsilon^{tor}=1$, 2, and 3, respectively. The negative $s(z)$ in the successive interfacial fluid layers after the first fluid layer suggests that a low degree of ordering, which may be related to the oblique packing of molecules, still occurs in these regions. It is noted that in case $\varepsilon^{tor}\geq 2kT_0$, the ordering parameter $\bar{s}(z)$ becomes almost zero at $z\simeq\lambda_1'\simeq\lambda_i+3$ ($i=A$ or B), for both solute and solvent molecules. This implies that the parallel ordering of molecules almost completely vanishes in the layer.

The ordering of rigid-chain molecules and the oscillation of the segmental density are attributed to the energy and the (negative) entropy effect. For the arrangement of rigid molecules, in the solid-fluid interface two opposite trends compete with each other. To achieve the maximum adsorption energy, chain molecules are strongly adsorbed and ordered on the solid surface. On the other hand, to gain the maximum conformational entropy, molecules tend to be oriented randomly. In the regions near the surface [$z<\lambda_i'$ (or λ_i for completely rigid-chain molecules)], the number of orientations is restricted. This will cause the loss of the conformational entropy and other entropies for chain molecules. Then chain molecules would rather avoid the solid surface. Obviously, these two effects become more pronounced when molecules become longer. In the first fluid layer, the adsorption is the dominant effect, and solute (or longer) molecules are adsorbed strongly on the solid surface for energic reasons. In order to release the maximum adsorption energy per molecule, most fluid molecules are oriented in directions parallel to the surface. In the successive liquid layers, the adsorption energy decreases considerably. The entropy effect then becomes relatively important. As a consequence, solute (or longer chain) molecules are repelled from these regions. Instead, these layers are preferentially filled with solvent (or shorter chain) molecules. At $z=\lambda_{min}\simeq\lambda_B'$ (or λ_B) the entropy effect of solvent molecules vanishes, and all conformations are possible. Then the space can be filled the best with solvent molecules. This causes a substantial depletion of solute molecules.

Similarly, the entropy effect of solute molecules vanishes at $z=\lambda_0$ (or $\lambda_{max}) \simeq \lambda'_A$ (λ_A), resulting in an increase of $\varphi_A(z)$. Chain conformations in interfacial regions and the relation to the energy and the entropy effect for the completely rigid-chain molecule system are illustrated in Fig. 9.

2. *Influences of various factors on the interfacial structure and properties*

As was shown in the last section, the exponential law is not valid for the description of the interfacial structure of rigid-chain molecule systems. However, C_l^* is still a key factor for understanding the solid-fluid interface, because the wetting condition and interfacial properties can in principle be described by this factor.

It can be seen from Fig. 10 that the change of the surface scaling factor C_l^* as a function of the segment number of chain molecules (or the carbon number of *n*-paraffin molecules) is shown, in the case that the solvent is given. (n-C_6 is chosen as the solvent in this case.) In general, the value of C_l^* decreases as the segment number increases. When the segment number becomes relatively large, C_l^* changes slowly. This is because with increasing carbon number, the difference between neighboring homologues of paraffin become smaller.

In spite of the segment number of molecules, the bulk concentration will also influence C_l^*. Figure 11 displays a relation between C_l^* and the concentration of solute. As can be seen, the dependence of C_l^* on the concentration is very weak. Unlike flexible-chain molecular systems presented in Fig. 3, the calculated C_l^*-φ_A curve for

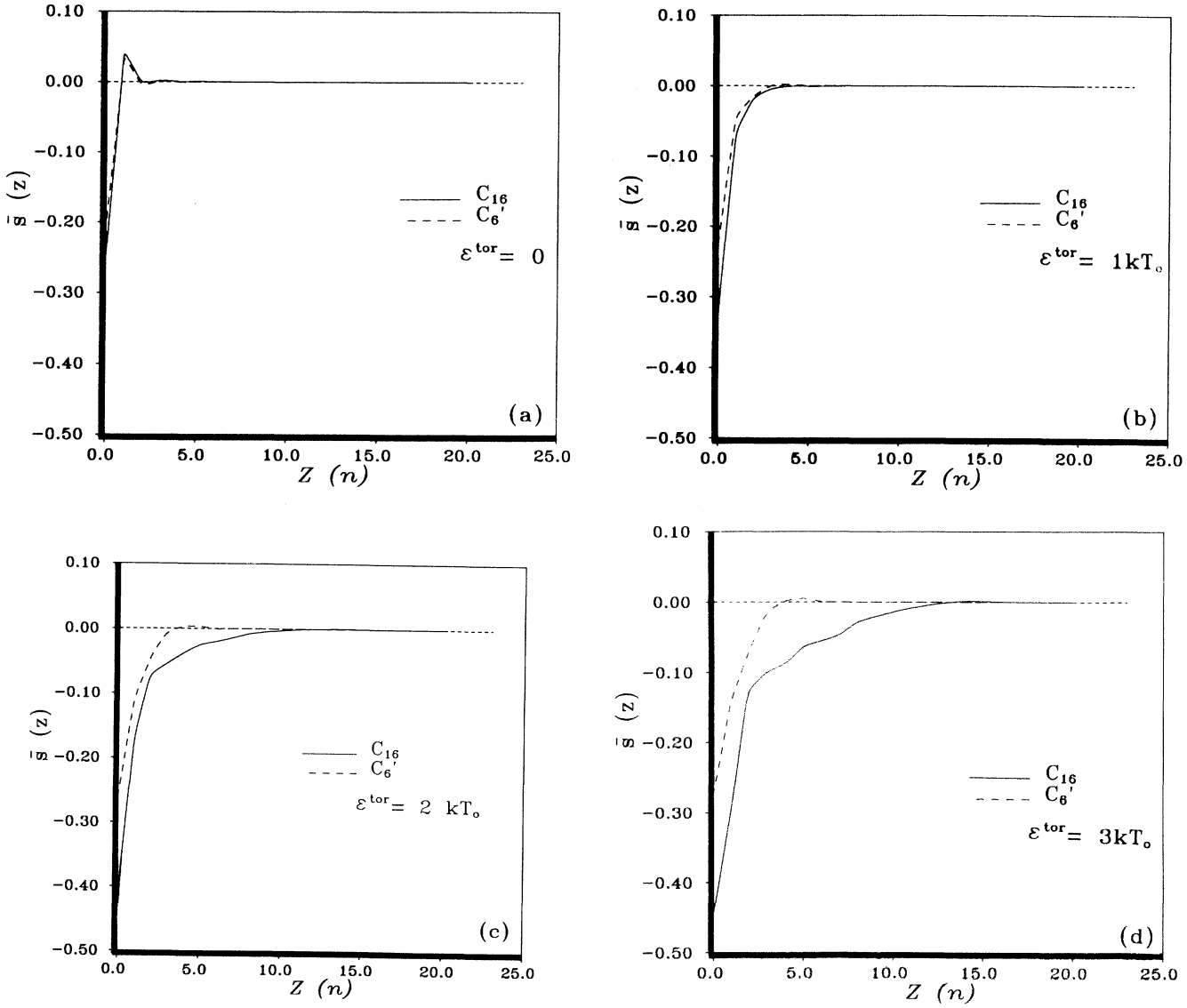

FIG. 8. The average order parameter $\bar{s}(z)$ of fluid molecules as a function of z for crystals in contact with a n-C_{16}–n-C_6 solution. $\varphi_A=0.1$. Molecules in the first fluid layer ($z=0$) are highly ordered in the case that $\varepsilon^{tor}>0$. It follows that the degree of the ordering drops drastically in the successive layers after the first fluid layers. (a)–(d) correspond to different ε^{tor}, respectively.

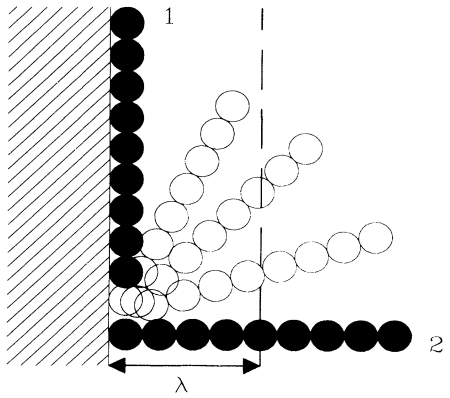

FIG. 9. Schematic illustration of chain conformations and in relation to the energy and the entropy effect at the surface. In the first fluid layer, the energy effect is dominant. Between the first fluid layer and the layer $z=\lambda$, the entropy effect becomes important. In the layer $z \geq \lambda$, the entropy effect almost vanishes. For more explanations, see the text. λ represents half of the chain length of molecules.

somewhat rigid-chain molecular systems can be fitted perfectly well with a parabolic curve with the maximum at $\varphi_A \simeq 0.5$.

The influence of the temperature on C_l^* is similar to the energy. For a given interfacial system, raising the temperature corresponds to increasing the influence of the entropy. This will reduce the effect of adsorption energy. Also, molecular chains become more flexible at a higher temperature because in this case the thermal energy may compensate the torsional energy. It follows that the adsorption of solute molecules on the solid surface becomes less pronounced. It can be seen from Fig. 12 that with increasing temperature, C_l^* increases correspondingly. As expected, at higher temperatures profiles of the segment density of paraffin molecules have a character similar to that of flexible-chain molecules.

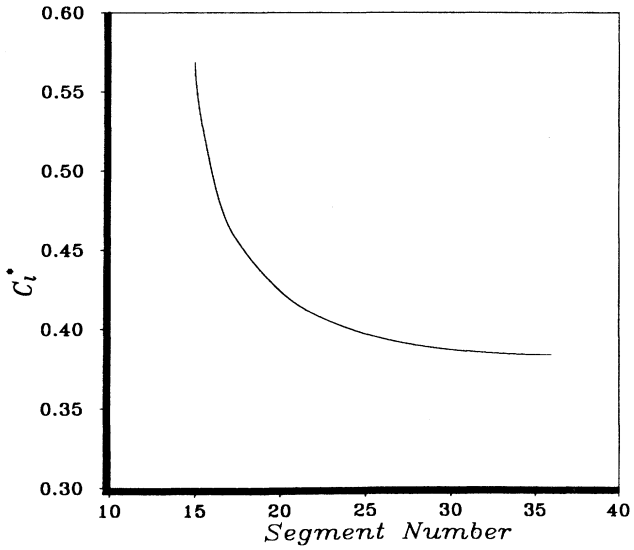

FIG. 10. The relation between the surface characteristic scaling factor C_l^* and the carbon number of paraffin molecules. This lattice structure is hexagonal: For the given solvent (n-C_6), the dependence of C_l^* on the chain length of solute molecules.

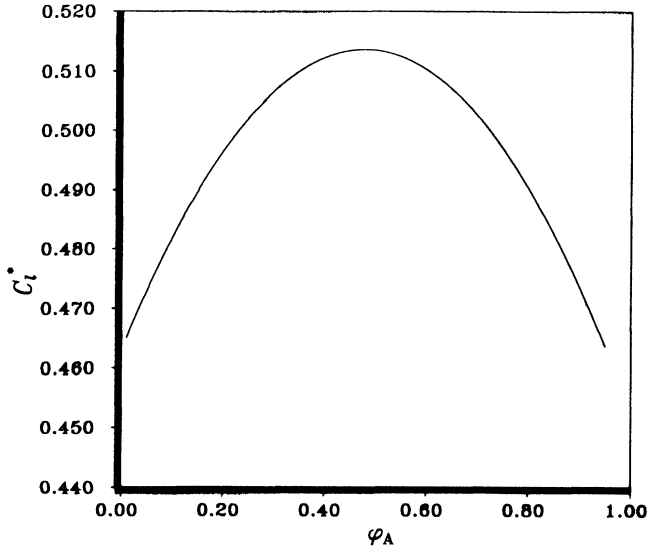

FIG. 11. The dependence of the sruface scaling factor C_l^* on the bulk concentration of solutions φ_A. The lattice structure is hexagonal. The curve of C_l^* have a parabolic shape with the maximum at $\varphi_A \simeq 0.5$.

In addition to other effects, crystal structures also influence C_l^*. In order to make a comparison between different structures, we will first define an orientation factor of crystal surfaces ξ_{hkl}.

According to the Hartman-Perdok theory [6,25], we know that each flat crystal surface has a certain attachment energy E_{hkl}^{att}. This is the energy released per structural unit when a new crystal slice is attached to the

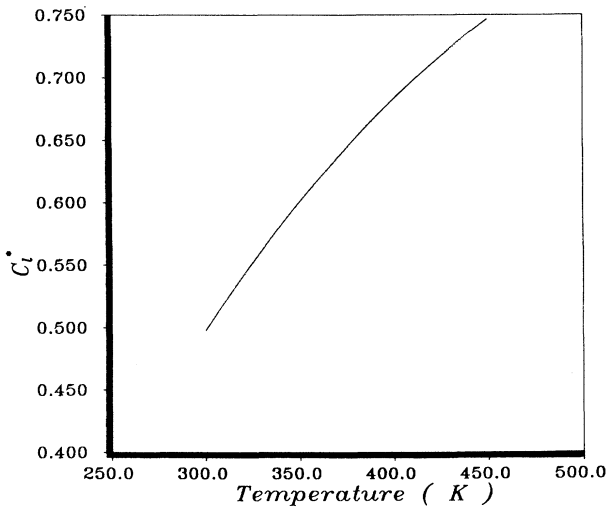

FIG. 12. The dependence of the surface scaling factor C_l^* on the temperature for the system of n-C_{25}–n-C_{12} solutions. The lattice structure is fcc.

TABLE I. Influence of different crystal structures on the surface scaling factor C_l^* for the system of n-C_{21} crystals in n-C_6 solutions. For this system, $\varphi_A = 0.1$, $\varepsilon^{tor} \simeq 2kT_0$, $\chi_{SA} = -1.269$, and $\chi_{SB} = -0.594$.

Crystal structure	$\{hkl\}$	ξ_{hkl} [a]	C_l^*
fcc	{100}	0.333	0.416
Hexagonal	{001}	0.250	0.485
bcc	{110}	0.250	0.485
Simple cubic	{100}	0.125	0.573

[a]The orientation factor ξ_{hkl} refers to crystals consisting of monomer units.

crystal surface. In relation to the crystallization energy (per structural unit), the attachment energy is expressed as

$$E^{cr} = E_{hkl}^{att} + E_{hkl}^{slice} , \tag{9}$$

where E_{hkl}^{slice} is the slice energy of crystal surfaces $\{hkl\}$ [6,25]. It can also be defined as the two-dimensional crystallization energy of a crystal slice with a thickness d_{hkl} for orientations $\{hkl\}$. Within this framework, the orientation factor of crystal surfaces $\{hkl\}\xi_{hkl}$ is defined as

$$\xi_{hkl} = E_{hkl}^{att}/(2E^{cr}) . \tag{10}$$

ξ_{hkl} is approximately proportional to the surface excess energy or the adsorption energy for a given system, and is used to characterize the anisotropy of bond energies of crystal structures. For different crystal structures, ξ_{hkl} will be different. It follows that for a given set of energy parameters and the bulk concentration, C_l^* will also be different. Table I shows that different structures affect C_l^* in the case of n-C_{21} crystals in n-C_6 solutions ($\varphi_A = 0.1$). It is explicit that for these crystal structures, ξ_{hkl} plays a key role in the determination of the value of C_l^*. For a given crystal structure, different crystal surfaces may also have different ξ_{hkl}. Then a similar influence can be expected. It can be seen from Table I that a larger ξ_{hkl} (or a larger E_{hkl}^{att}) corresponds to a lower C_l^*. This can be interpreted as follows. As mentioned above, the surface excess energy or the adsorption energy of a crystal surface is proportional to E_{hkl}^{att} or ξ_{hkl}. Henceforth, the enhancement of ξ_{hkl} (or E_{hkl}^{att}) will lead to an increase in the number of preferentially adsorbed molecules in the first fluid layer adjacent to the solid phase. Since for paraffin systems the more than equivalent wetting occurs ($C_l^* < 1$), solute molecules are the preferentially adsorbed molecules. It therefore follows from Eq. (4) that C_l^* will decrease further from unity.

C. Comparison with experimental data

We know from the foregoing discussions that C_l^* can be evaluated from the calculated $\varphi_A(0)$ and the φ_A. However, from an experimental point of view, C_l^* can also be determined, as was mentioned in Sec. II A. For the bulk phase the exchange energy in direction i for the bulk phase ϕ_i can be calculated from the dissolution enthalpy Δh_{diss}, based on Eqs. (2) and (3). On the other hand, the corresponding value at the interface $\phi_i(0)$ can precisely be measured from surface roughening experiments according to Eq. (5) or obtained from the kinetic data of crystals growth kinetics according to Eqs. (6) and (6′). C_l^* is then obtained from Eq. (4). As a comparison, we list in Table II the calculated and experimental values of C_l^* for various paraffin systems, together with other relevant data.

It is interesting to see that although different experimental methods are used to measure C_l^* for various systems, the calculated values of C_l^* agree well in every case with the experimental ones. It can also be seen from the above-mentioned discussions that C_l^* is directly associated with the whole interfacial structure. Any change of C_l^* corresponds to a certain change in the interfacial structure. Therefore, as a key factor, C_l^* plays an important role in characterizing the interfacial structure. From this point of view our results are quite convincing.

Another important issue described earlier is the ordering of paraffin molecules in the first fluid layer. This has also been justified by experiments. It is known from recent scanning-tunneling-microscopic (STM) experiments [28] that once paraffin solutions are applied to a graphite substrate, highly ordered monomolecular layers occur at the graphite surface. This is consistent with our calculated results [see Fig. 8(c)]. We notice that investigations on the ordered structure of paraffins at the solid-fluid interface can offer physical insight to the molecule behavior at

TABLE II. Calculated and experimental values of the surface scaling factor C_l^* for various paraffin solution systems.

Solutions	φ_A [a]	$\varphi_A(0)$	C_l^*(calc.)	C_l^*(expt.)
n-C_{21}–n-C_6	0.100	0.519	0.406	0.414[b]
n-C_{25}–n-C_6	0.100	0.579	0.382	0.373[b]
n-C_{16}–n-C_6	0.820	0.911	0.457	0.460[b]
n-C_{36}–Pet. eth[c]	0.100	~0.489	~0.440	0.457[d]

[a] φ_A is the bulk concentration in which C_l^*(expt.) was determined.
[b]Pet. eth. (petroleum ether) is a mixture of different components. In our calculations, an average is made for several n-paraffin solution systems.
[c] C_l^*(expt.) determined according to Eqs. (4) and (5).
[d] C_l^*(expt.) calculated according to Eqs. (4), (6), and (6′), based on the data quoted from Ref. [29].

the interface. This will help us to understand the influence of solvents and impurities on the morphology of crystals, then lead to the molecular design of tailor-made additives. Without doubt, further investigations from theoretical and experimental points of views are needed. We expect that significant more progress can be made in the near future.

IV. SUMMARY AND CONCLUSIONS

The structure and some thermodynamic properties of the solid-fluid interface were investigated using the SCF calculations. For systems of completely flexible-chain molecules, the exponential law is valid, and the structure of the interface can be characterized by two key factors: C_l^* and n^*. For somewhat rigid-chain molecule systems, the ordering and the layering of molecules at the interface become a crucial issue. The oscillation of segmental-density profiles has the one-to-one relation with the chain length of molecules. In addition to C_l^*, the interfacial structure of rigid molecule systems is determined in a qualitative way by λ'_A and λ'_B. C_l^* determines the wetting condition at the solid surface, while λ'_A and λ'_B may characterize the oscillation of profiles of the segmental density. When the structure of molecules in interfacial systems are changed, the oscillation and the values of C_l^* will be altered accordingly. Moreover, C_l^* depends directly on bulk properties, such as the bulk concentration and χ_{si}, and also on the crystal structure or orientations of crystal surfaces.

ACKNOWLEDGMENTS

We are very much indebted to Dr. F. A. M. Leermakers, Professor Dr. G. J. Fleer, and Drs. C. Meijer for fruitful discussions and providing the SCF computer program for our calculations. We would also like to thank Drs. R. Geertman for technical support and Dr. H. Meekes for a critical reading of the manuscript. This research was supported by Shell Netherlands B.V.

[1] X. Y. Liu and P. Bennema, J. Chem. Phys. **97**, 3600 (1992).
[2] X. Y. Liu and P. Bennema, J. Chem. Phys. **98**, 5863 (1993).
[3] X. Y. Liu, Surf. Sci. **290**, 403 (1993).
[4] X. Y. Liu, J. Chem. Phys. **98**, 8154 (1993).
[5] P. Bennema, X. Y. Liu, K. Lewtas, R. D. Tack, J. J. M. Rijpkema, and K. J. Roberts, J. Cryst. Growth **121**, 679 (1992).
[6] P. Bennema, in *Handbook on Crystal Growth,* edited by D. T. J. Hurle (North-Holland, Amsterdam, in press).
[7] X. Y. Liu, P. Bennema, and J. P. van der Eerden, Nature (London) **356**, 778 (1992).
[8] X. Y. Liu, Phys. Rev. B **48**, 1825 (1993).
[9] X. Y. Liu, P. van Hoof, and P. Bennema, Phys. Rev. Lett. **71**, 109 (1993).
[10] J. Q. Broughton and F. F. Abraham, Chem. Phys. Lett. **71**, 456 (1980).
[11] J. Q. Broughton and G. H. Gilmer, J. Chem. Phys. **79**, 5095 (1983); **79**, 5105 (1983); **79**, 5119 (1983); **84**, 5741 (1986); **84**, 5749 (1986); **84**, 5759 (1986).
[12] A. Bonissent, in *Interfacial Aspects of Phase Transformation,* edited by B. Mutaftschiev (Reidel, Dordrecht, 1982).
[13] U. Landman, C. S. Brown, and C. L. Cleveland, Phys. Rev. Lett. **45**, 2032 (1980).
[14] E. T. Chen, R. N. Barnett, and U. Landman, Phys. Rev. B **40**, 924 (1989).
[15] J. D. Weeks, J. Chem. Phys. **67**, 3106 (1977).
[16] O. Guiselin, L. T. Lee, B. Farnoux, and A. Lapp, J. Chem. Phys. **95**, 4632 (1991).
[17] H. K. Christenson, W. R. Gruen, R. G. Horn, and J. N. Israelachvili, J. Chem. Phys. **87**, 1834 (1987).
[18] (a) T. Pakula, J. Chem. Phys. **95**, 4685 (1991); (b) T. Pakula and E. B. Zhulina, *ibid.* **95**, 4691 (1991).
[19] T. K. Xia, Jia Ouyang, M. W. Ribarsky, and U. Landman, Phys. Rev. Lett. **69**, 1967 (1992).
[20] J. M. H. M. Scheutjens and G. J. Fleer, J. Phys. Chem. **83**, 1619 (1979); **84**, 178 (1979).
[21] O. A. Evers, J. M. H. M. Scheutjens, and G. J. Fleer, Macromolecules **23**, 5221 (1990); **24**, 5558 (1991).
[22] J. M. H. M. Scheutjens and G. J. Fleer, Macromolecules **18**, 1882 (1985).
[23] F. A. M. Leermakers and J. M. H. M. Scheutjens, J. Chem. Phys. **89**, 3264 (1988); **89**, 6912 (1988); **93**, 7417 (1989).
[24] S. R. Fowler and E. A. Guggenheim, *Statistical Thermodynamics* (Cambridge University Press, London, 1960).
[25] P. Bennema and J. P. van der Eerden, in *Morphology of Crystals, Part A,* edited by I. Sunagawa (Terra Scientific, Tokyo, 1987), p. 1.
[26] M. G. Broadhurst, J. Res. Natl. Bur. Stand. A **66**, 241 (1962).
[27] A. S. Wingrove and R. L. Caret, *Organic Chemistry* (Harper & Row, New York, 1981).
[28] M. Couto, X. Y. Liu, H. Meekes, and P. Bennema (unpublished).
[29] B. Simon, A. Grassi, and R. Boistelle, J. Cryst. Growth **26**, 77 (1974).